MICROBOONE-NOTE-1104-PUB

PROGRESS TOWARDS AN INVESTIGATION OF THE MINIBOONE LOW ENERGY EXCESS USING NEUTRAL-CURRENT DELTA-LIKE SINGLE PHOTONS IN MICROBOONE WITH WIRE-CELL 3D RECONSTRUCTION ALGORITHMS

May 29, 2022

The MicroBooNE Collaboration

microboone_info@fnal.gov

Abstract

This note presents progress towards a Neutral-Current (NC) Delta-like single photon search in MicroBooNE using Wire-Cell 3D reconstruction and pattern recognition algorithms. This analysis will help address the question of the MiniBooNE Low Energy Excess (LEE) [1]. The selections are similar to the previously published Pandora-based single photon selections [2] in many ways, but here we use independent reconstruction and selection tools and examine a larger phase space (including charged pions and multiple protons). In the future, we will significantly reduce systematic uncertainties via the use of constraining sideband observations in order to statistically test specific models of the MiniBooNE LEE.

Contents

1 INTRODUCTION

MicroBooNE [3] is an experiment using a Liquid Argon Time Projection Chamber (LArTPC) in the Booster Neutrino Beam (BNB) at Fermilab, designed in part to probe a low energy electromagnetic excess (LEE) observed by the MiniBooNE experiment in the same neutrino beam [1]. The use of a LArTPC enables discrimination between electrons and photons as well as a detailed view of hadronic activity, allowing an investigation of the origin of the MiniBooNE LEE.

While MicroBooNE had several electron-like LEE analyses working in parallel and doing various consistency checks, Ref. [2] was the only LEE analysis looking in the photon channel. We determined that an additional examination of the photon channel targeting NC Delta radiative decays could be completed using existing Wire-Cell tools.

The goal of this note is to summarize progress towards an NC Delta-like single photon search using Wire-Cell reconstruction and pattern recognition [4, 5]. This analysis can function as a cross-check of the previously published Pandora-based analysis [2], and will further test the NC Delta hypothesis as the origin of the MiniBooNE excess. This analysis will also take a closer look at the 1g0p channel (a single photon shower with no visible protons) with significantly higher efficiency and purity than the previously published Pandora-based analysis [2].

2 EVENT SELECTION

All the tools used for this analysis are described in detail in Refs. [6, 7].

Events in our selection must have all reconstructed charge fully contained in the fiducial volume (FV), they must pass the Wire-Cell generic neutrino selection [8], they must have at least one reconstructed shower, and they must pass our NC Delta Boosted Decision Tree (BDT) cut. We split our events into two samples: zero reconstructed protons (0p), and one or more reconstructed protons (Np). For this purpose, we count both primary and non-primary protons with reconstructed kinetic energy greater than 35 MeV. This method of 0p/Np separation is the same one which has been used in Ref. [6]. 1gNp refers to selected events with at least one reconstructed proton, 1g0p refers to selected events with no reconstructed protons, and 1gXp refers to selected events with any number of reconstructed protons (including zero protons). 1gNp, 1g0p, and 1gXp each allow any number of reconstructed charged pions.

The NC Delta BDT was trained on 181,492 simulated events, with NC $\Delta \rightarrow N\gamma$ events as signal. We use 341 variables which were previously used in [6]. The training was done using

	Wire-Cell 1gNp	Pandora 1g1p	Wire-Cell 1g0p	Pandora 1g0p
NC $\Delta \rightarrow N\gamma$ eff.	4.09%	3.99%	8.78%	5.29%
NC $\Delta \rightarrow N\gamma$ pur.	10.4%	15.3%	7.97%	3.81%

Table 1: Efficiency and purity summary and comparison with the previous Pandora single photon analysis [2]. Note that unlike in this analysis, the Pandora analysis did not attempt to reconstruct any events containing visible charged pions, or any events with more than one visible proton. Also note that the Pandora analysis used a slightly larger volume (3 cm in each direction) of possible true neutrino vertices to define signal events in the efficiency calculation.

XGBoost [9] and using the same training parameters as were used for the charged-current electron neutrino BDT training [6].

Throughout this note, we define the signal as all true NC $\Delta \rightarrow N\gamma$ events with a true neutrino vertex in the fiducial volume. Note that signal events can contain any number of true or reconstructed protons or pions. Efficiency is defined as a fraction, with the numerator being all true signal Monte-Carlo events which enter the selection, and the denominator being all true signal Monte-Carlo events. Purity is defined as a fraction, with the numerator being all true signal Monte-Carlo events which enter the selection, and the denominator being all events in the selection. Table 1 shows a summary of the efficiency and purity, and a comparison with the previously published Pandora-based single photon analysis [2].

In Fig. 1, we show the efficiency as a function of the primary photon true angle and energy.

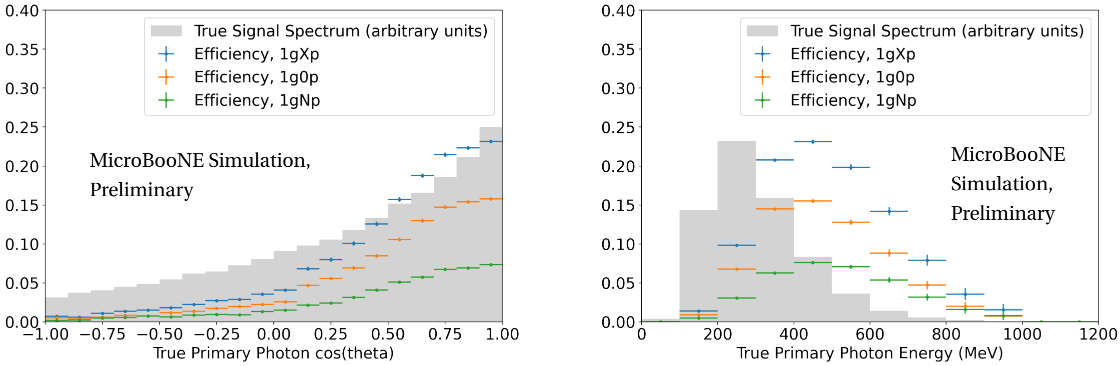

Figure 1: Left: Selection efficiency as a function of true primary photon angle. Right: Selection efficiency as a function of true primary photon energy. 1gXp refers to events with any number of reconstructed protons, 1g0p refers to events with zero reconstructed protons, and 1gNp refers to events with at least one reconstructed proton.

To obtain systematic uncertainties, we follow the same procedure as was used in Ref. [6]. This procedure includes considerations of the BNB flux uncertainties, neutrino-argon interaction cross section uncertainties, hadron-argon interaction uncertainties, detector response uncertainties, and Monte Carlo statistical uncertainties. Additional uncertainties related to higher mass resonances, photonuclear absorption, and coherent single photon production have been considered and determined to be negligible in this analysis.

In this note, we show unconstrained predictions and uncertainties. Previous MicroBooNE LEE analyses [2, 10] as well as the MiniBooNE electron-like analysis [1] made use of data observations in sideband channels to constrain the prediction, updating the central value and reducing systematic uncertainties. We plan to do the same for this analysis in the future.

3 Predictions

In this section, we show several distributions of predicted events.

3.1 BDT Score

In Fig. 2, we show the NC Delta BDT score distributions for simulated events which pass Wire-Cell generic neutrino selection and have at least one reconstructed shower.

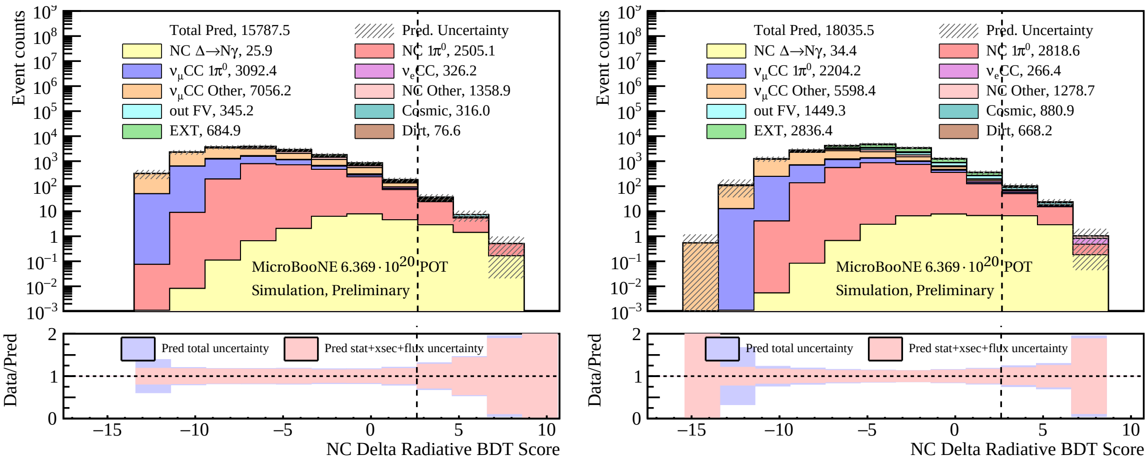

Figure 2: NC Delta Radiative BDT score distributions. The prediction and uncertainties shown here are unconstrained. Shown here are all fully contained events which pass WC generic neutrino selection and have at least one reconstructed shower. Events with a score greater than 2.61 (indicated by the dashed line) are included in our NC Delta selection. Left: events with one or more reconstructed protons. Right: events with zero reconstructed protons.

3.2 One Bin

Figure 3 shows the one bin result for each selection.

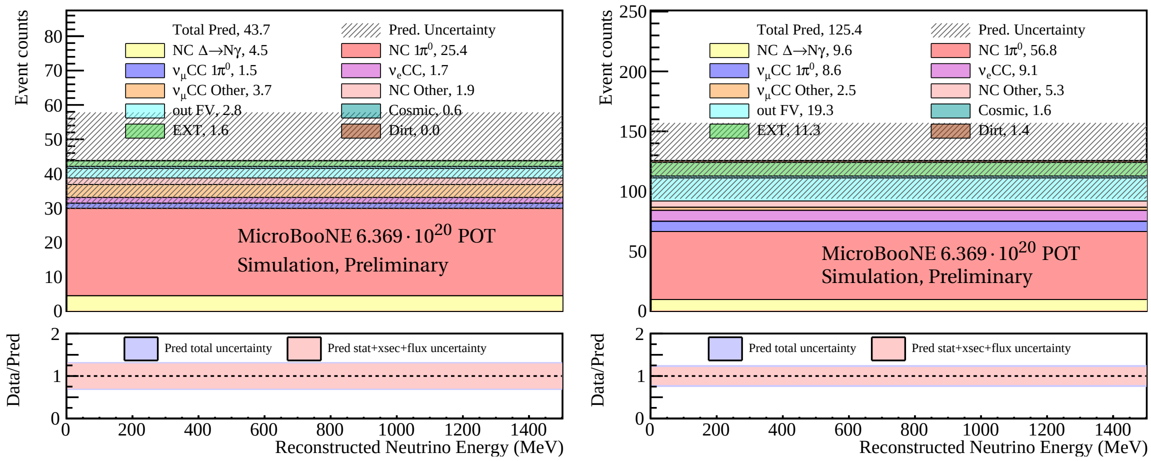

Figure 3: One bin selections. The prediction and uncertainties shown here are unconstrained. Left: events with one or more reconstructed protons. Right: events with zero reconstructed protons.

3.3 Energy

Figures 4 and 5 show the reconstructed neutrino energy and reconstructed shower energy for each selection.

Note that "reconstructed neutrino energy", calculated as described in [7], is really an estimate of the energy transferred by the neutrino to the nucleus for neutral current interactions. We do not consider the energy of the exiting neutrino in this variable.

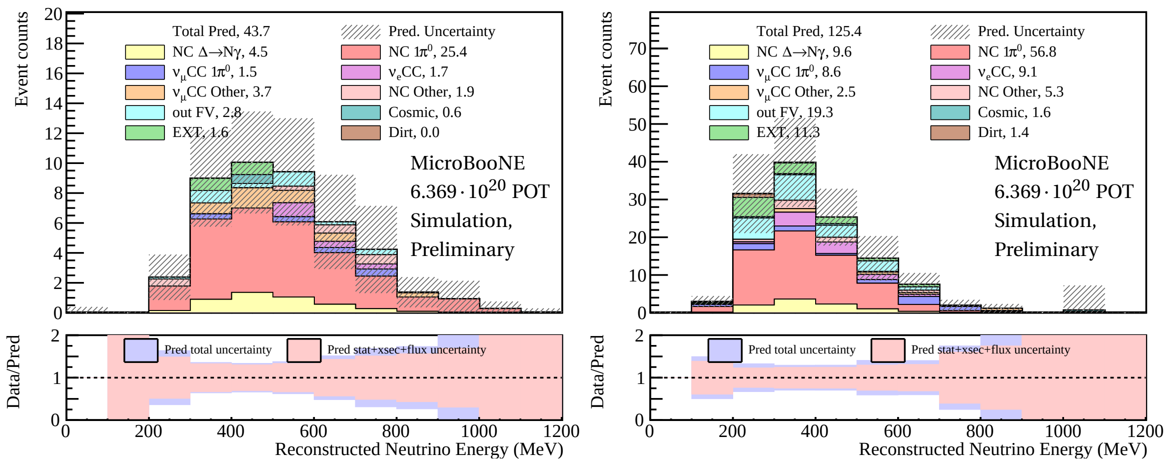

Figure 4: Reconstructed neutrino energy distributions. The prediction and uncertainties shown here are unconstrained. Left: events with one or more reconstructed protons. Right: events with zero reconstructed protons.

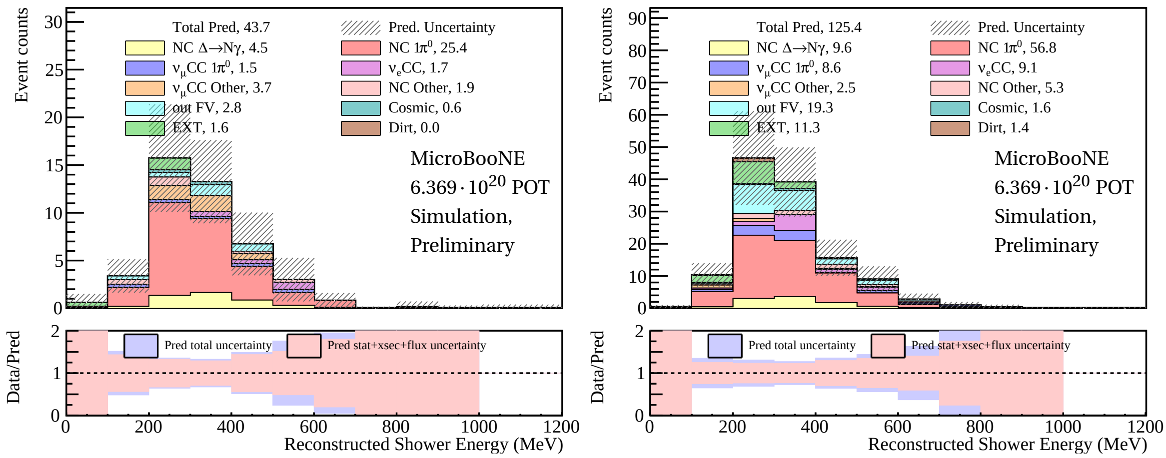

Figure 5: Reconstructed shower energy distributions. The prediction and uncertainties shown here are unconstrained. Left: events with one or more reconstructed protons. Right: events with zero reconstructed protons.

3.4 Shower Angle

Figure 6 shows the reconstructed shower angle distribution for each selection.

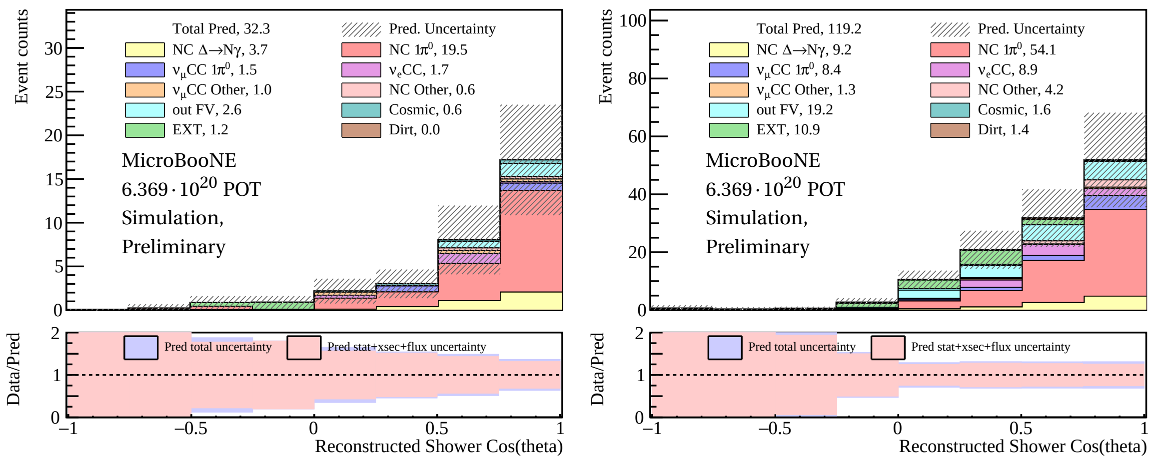

Figure 6: Cosine of the angle between the reconstructed primary shower direction and the beam direction. The prediction and uncertainties shown here are unconstrained. Left: events with one or more reconstructed protons. Right: events with zero reconstructed protons.

3.5 Particle Multiplicity

As shown in Figs. 7 and 8, our 1gNp prediction is dominated by events with just one reconstructed proton, and both the 1gNp and 1g0p predictions are dominated by events with zero reconstructed charged pions.

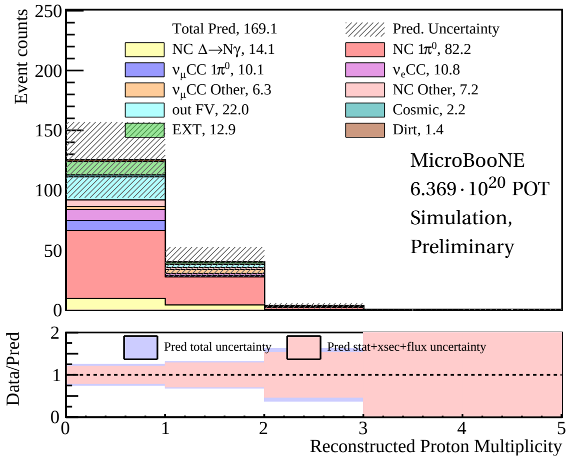

Figure 7: Number of reconstructed protons, with a 35 MeV reconstructed energy threshold, in the 1gXp selection (1g0p and 1gNp combined). The prediction and uncertainties shown here are unconstrained.

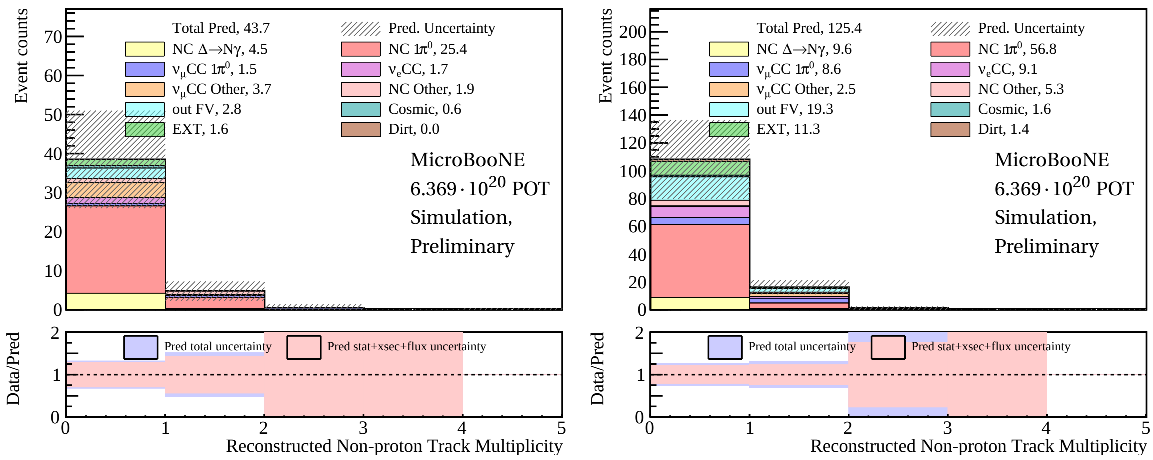

Figure 8: Number of reconstructed non-proton tracks (mostly charged pions), with a 10 MeV reconstructed energy threshold. The prediction and uncertainties shown here are unconstrained. Left: 1gNp selection. Right: 1g0p selection.

4 Comparison with MiniBooNE

Comparisons between MicroBooNE and MiniBooNE are complicated by many factors. For example, the two experiments use different target nuclei, different reconstruction techniques, and different cross section predictions.

Below, we show some additional ways to compare our shower energy and angle predictions with MiniBooNE.

4.1 E_ν^{QE} Distribution

In Fig. 9, we plot E_ν^{QE}. This variable gives an estimate of the neutrino energy in a charged-current quasi-elastic electron neutrino interaction. This variable is purely a function of the reconstructed shower energy and angle, with no proton or pion information considered.

Although we do not investigate charged-current quasi-elastic interactions in this analysis, this variable is useful for comparison because it is the primary variable that the MiniBooNE experiment uses to investigate the low energy excess.

The electron mass is assumed for all showers, and the neutron binding energy is set at 30 MeV. More information about this type of energy reconstruction can be found in [11].

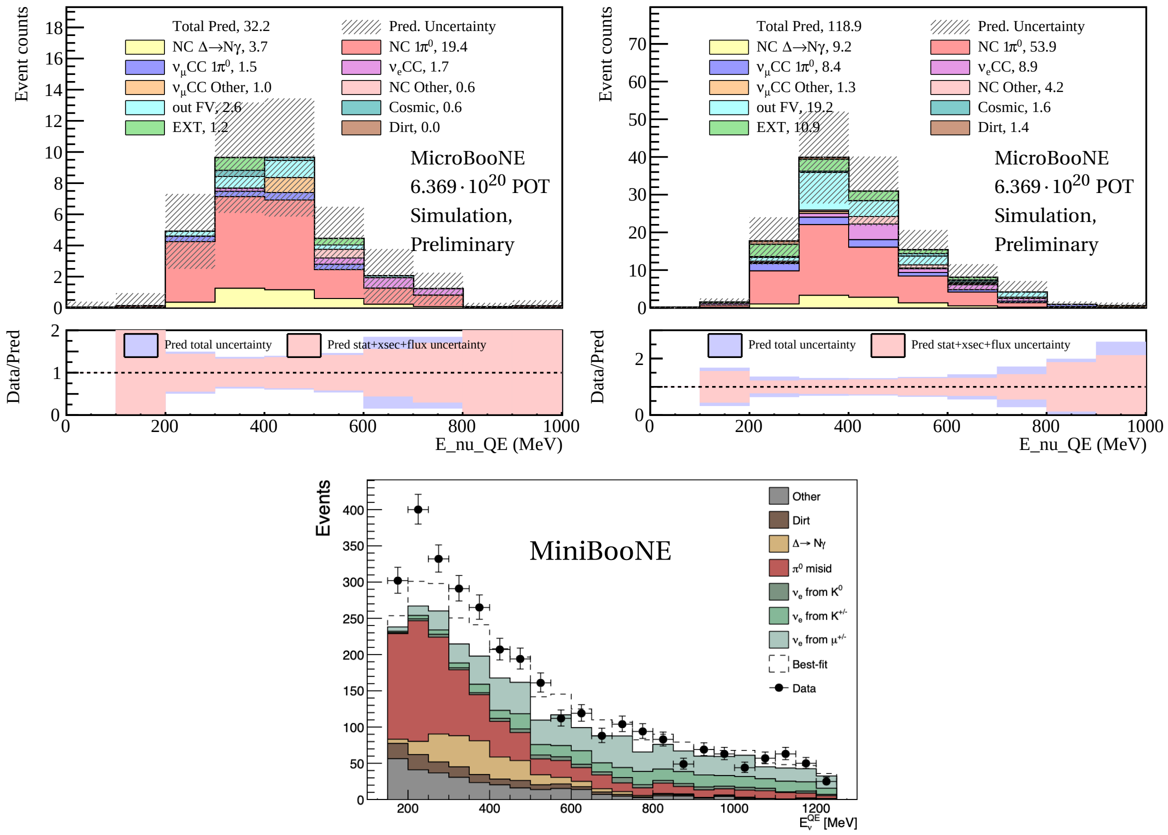

Figure 9: E_ν^{QE} distributions. The MicroBooNE prediction and uncertainties shown here are unconstrained. Left: events with one or more reconstructed protons. Right: events with zero reconstructed protons. Bottom: MiniBooNE $18.75 \cdot 10^{20}$ POT neutrino mode electron-like selection from [1]

4.2 2D Energy-Angle Distribution

Here we examine the 2D distribution of shower energy and angle. MiniBooNE cannot easily reconstruct low energy protons or pions, so here we show the 1gXp selection which includes any number of reconstructed protons or pions.

Figure 10 shows that we investigate roughly the same phase space in reconstructed shower energy and angle as the MiniBooNE LEE.

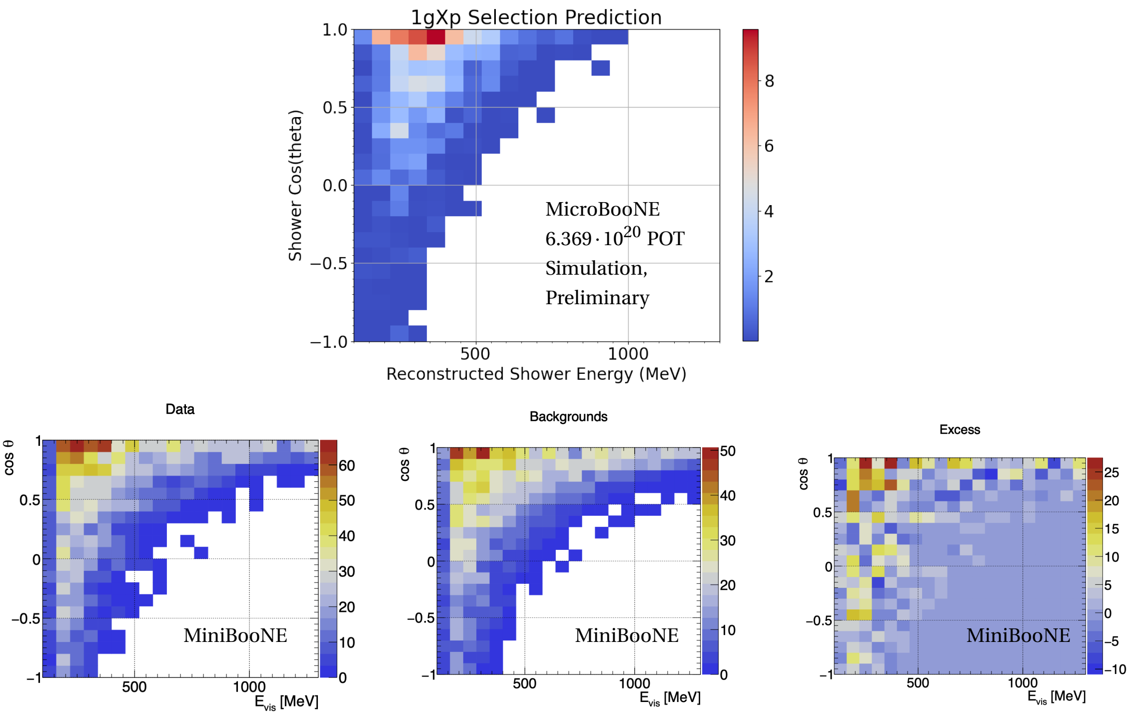

Figure 10: 2D Energy-Angle distribution. The MicroBooNE prediction shown here is unconstrained. The z axis corresponds to the number of events. Top: MicroBooNE Wire-Cell $6.369 \cdot 10^{20}$ POT 1gXp prediction. Bottom: MiniBooNE $18.75 \cdot 10^{20}$ POT neutrino mode electron-like selection from Ref. [1]. Left: Data events. Middle: Predicted events. Right: Excess events (data - prediction).

5 SUMMARY

In this analysis, we examine NC Delta-like single photon events in MicroBooNE. For single photon showers with no visible hadronic activity, this is the most efficient and most pure MicroBooNE selection released.

This note presents a first look at our selections. The analysis will ultimately make use of sidebands to constrain these predictions and significantly reduce systematic uncertainties, a technique applied by the previous MicroBooNE NC $\Delta \to N\gamma$ analysis [2], and by the MiniBooNE experiment [1].

In the future, we will use these selections to perform an LEE strength fitting procedure similar to that in Ref. [2], which will let us analyze consistency with a nominal prediction and a prediction corresponding to the MiniBooNE LEE under an NC $\Delta \rightarrow N\gamma$ hypothesis. Thinking beyond an NC $\Delta \rightarrow N\gamma$ hypothesis, more work is ongoing to investigate how these selections can constrain different theoretical models of the MiniBooNE low energy excess, including beyond-the-standard-model sources of photons or e^+e^- pairs.

A Selected Data Event Displays

In Fig. 12, we show two candidate selected single photon events from MicroBooNE data. Displayed is the 3D trajectory fitted space points, where color corresponds to dE/dx.

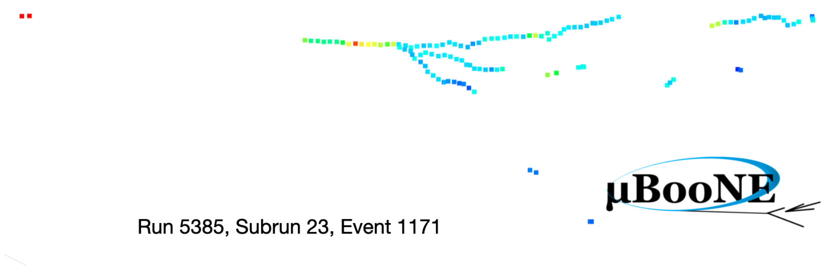

Figure 11: 1gNp candidate data event, reconstructed as one 60 MeV proton and one 252 MeV photon.

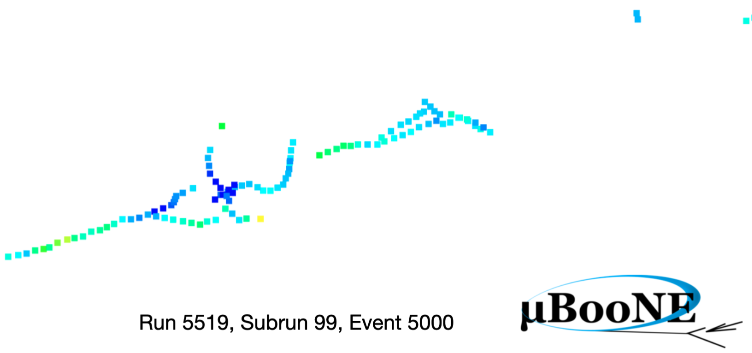

Figure 12: 1g0p candidate data event, reconstructed as one 246 MeV photon.

REFERENCES

[1] MiniBooNE Collaboration. Updated miniboone neutrino oscillation results with increased data and new background studies. *Phys. Rev. D*, 103:052002, Mar 2021.

[2] MicroBooNE Collaboration. Search for neutrino-induced neutral-current Δ radiative decay in microboone and a first test of the miniboone low energy excess under a single-photon hypothesis. *Phys. Rev. Lett.*, 128:111801, Mar 2022.

[3] MicroBooNE Collaboration. Design and Construction of the MicroBooNE Detector. *JINST*, 12(02):P02017, 2017.

[4] MicroBooNE Collaboration. Neutrino event selection in the MicroBooNE liquid argon time projection chamber using wire-cell 3d imaging, clustering, and charge-light matching. *Journal of Instrumentation*, 16(06):P06043, jun 2021.

[5] X. Qian, C. Zhang, B. Viren, and M. Diwan. Three-dimensional imaging for large LArTPCs. *Journal of Instrumentation*, 13(05):P05032–P05032, may 2018.

[6] MicroBooNE Collaboration. Search for an anomalous excess of inclusive charged-current ν_e interactions in the microboone experiment using wire-cell reconstruction, 2021. arxiv:2110.13978.

[7] MicroBooNE Collaboration. Wire-cell 3d pattern recognition techniques for neutrino event reconstruction in large LArTPCs: algorithm description and quantitative evaluation with MicroBooNE simulation. *Journal of Instrumentation*, 17(01):P01037, Jan 2022.

[8] MicroBooNE Collaboration. Cosmic ray background rejection with wire-cell lartpc event reconstruction in the microboone detector. *Phys. Rev. Applied*, 15:064071, Jun 2021.

[9] Tianqi Chen and Carlos Guestrin. XGBoost: A Scalable Tree Boosting System. 2016. arxiv:1603.02754.

[10] MicroBooNE Collaboration. Search for an excess of electron neutrino interactions in microboone using multiple final state topologies, 2021. arxiv:2110.14054.

[11] Olga Lalakulich, Ulrich Mosel, and Kai Gallmeister. Energy reconstruction in quasielastic scattering in the miniboone and t2k experiments. *Physical Review C*, 86, 08 2012.